Data completion method for the characterization of sound source in confined domain

Alexandre Garcia, Christophe Langrenne

ACOUSTICS 2012

Data completion method for the characterization of sound source in confined domain

A. Garcia and C. Langrenne

Conservatoire National des Arts et Métiers, 292 rue Saint-Martin 75141 Paris Cedex 03
alexandre.garcia@cnam.fr

In the present paper, we present a Steklov-Poincaré formulation, in order to solve the inverse problem of acoustic source reconstruction in a confined domain [1, 2]. The solution is obtained by the resolution of the Helmholtz equation on an empty domain bounded by the union of the measurement surface and the surface of the vibrating structure. The difference between classical methods (NAH) and this Data Completion Method (DCM) is that Cauchy data (acoustic pressures and velocities) have to be known on the measurement surface to recover data on the remaining boundary. The DCM allows one to solve the inverse problem, even with acoustic perturbations due to sources in the exterior domain, or due to measurements in a confined domain. Simulation and experimental results are presented.

1 Introduction

In the last three decades, the resolution of the acoustic inverse problem has become very popular. The vibro-acoustic problem consists in recovering the acoustic quantities on a vibrating structure using near-field pressure measurements. This problem is an "ill-posed" problem in the sense of Hadamard, especially because a small error on data provides erratic solutions. In order to solve this problem, several approaches have been developed. Recently, Wu presented an overview of acoustic imaging methods and their associated regularization techniques [3]: near-field acoustical holography (NAH), inverse boundary element method (IBEM), least-square method (LSM)...

These techniques only require the knowledge of the pressure field (or velocity) on a Γ^m surface surrounding the source. Multiple data acquisition systems, with an antenna of two microphonic probes or pressure/velocity probes, allow us to access not only to the pressure, but also to the acoustic velocity on a surface. When these data are available, the acoustic inverse problem can be viewed as a data completion problem for the Helmholtz equation. This method is based on integral formulations, solved by boundary element method (BEM).

The Data Completion Method (DCM) appeared recently in acoustics, using a measurement surface Γ^m surrounding the source surface Γ^u (see figure 1) [1, 2]. The major drawback of this configuration is that one needs to mesh all the source surface, which can be time consuming if the size is large. In this paper, the DCM is adapted to the configuration of the figure 2 where only a part of the source (Γ^u) has to be recovered .

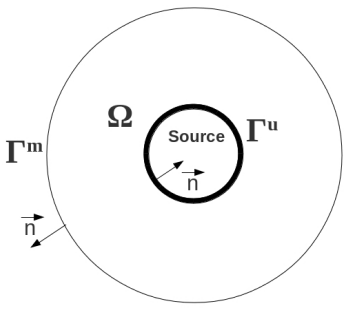

Figure 1: Problem configuration 1

2 Data Completion Method (DCM)

For a time-harmonic disturbance of pulsation ω, the Helmholtz-Kirchhoff integral is written on the surface $\Gamma = \Gamma^m \cup \Gamma^u$ (see figure 2):

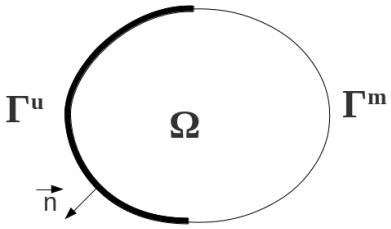

Figure 2: Problem configuration 2

$$-\iint_\Gamma [p(\vec{s'})\partial_n G(\vec{s},\vec{s'}) - \partial_n p(\vec{s'})G(\vec{s},\vec{s'})]d\Gamma = \frac{\Omega^-(\vec{s})}{4\pi}p(\vec{s}), \tag{1}$$

where $\vec{s}$ is a point on the surface Γ. The free space Green's function is $G(\vec{s},\vec{s'}) = e^{ikS}/(4\pi S)$, with $S = |\vec{s'} - \vec{s}|$ and Ω^- is the interior solid angle coefficient given by the following integral:

$$\Omega^- = -\iint_\Gamma \partial_n\Big(\frac{1}{S}\Big)d\Gamma. \tag{2}$$

The integral eq. (1) links together the acoustic pressure $p(\vec{s})$ and the normal gradient $\partial_n p(\vec{s})$ on the surface Γ. For the numerical implementation, the continuous integral is discretized on a mesh with an isoparametric formulation [4]. Then, vectors $\mathbf{p}$ and $\partial_\mathbf{n}\mathbf{p}$ are defined by:

$$\mathbf{p} = \begin{pmatrix}\mathbf{p^m}\\ \mathbf{p^u}\end{pmatrix} \qquad \partial_\mathbf{n}\mathbf{p} = \begin{pmatrix}\partial_\mathbf{n}\mathbf{p^m}\\ \partial_\mathbf{n}\mathbf{p^u},\end{pmatrix}$$

where $\mathbf{p^m}$ and $\partial_\mathbf{m}\mathbf{p^m}$ are the measured pressures and gradients on Γ^m, and $\mathbf{p^u}$ and $\partial_\mathbf{n}\mathbf{p^u}$ are the unknowns on Γ^u.

Using a Steklov-Poincaré formulation described in paper [2], one has to resolve to the following system:

$$\mathbf{F}\partial_\mathbf{n}\mathbf{p^u} = \mathbf{b}, \tag{3}$$

where $\mathbf{F}$ is the Steklov-Poincaré operator which only depends on the geometry of the discretized surface Γ, and $\mathbf{b}$ is a vector which is related to the geometry and to the measured acoustic quantities $\mathbf{p^m}$ and $\partial_\mathbf{n}\mathbf{p^m}$. This operator is "ill-conditioned" and a regularization technique must be used to find a realistic solution. We use standard Tikhonov and the "L-curve" methods to find the optimal regularization parameter [5].

3 Active intensity vector

Once vector $\partial_\mathbf{n}\mathbf{p^u}$ is known, the pressure $\mathbf{p^u}$ can be found with equation (1). Since the domain Ω is empty, one can calculate the pressure and the three components of the gradient vector for $\vec{r} \in \Omega$ with the discrete forms of equations:

$$p(\vec{r}) = -\iint_{\Gamma} [p(\vec{s'})\partial_n G(\vec{r},\vec{s'}) - \partial_n p(\vec{s'} G(\vec{r},\vec{s'})]d\Gamma, \quad (4)$$

and

$$\partial_i p(\vec{r}) = -\iint_{\Gamma} [p(\vec{s'})\frac{\partial^2}{\partial_n \partial_i} G(\vec{r},\vec{s'}) - \partial_n p(\vec{s'})\partial_i G(\vec{r},\vec{s'})]d\Gamma. \quad (5)$$

where i is one of the three components x, y or z.

The i component of the active intensity is given by:

$$I_i(\vec{r}) = \frac{1}{2}\Re e\Big\{p(\vec{r})\Big(\frac{\partial_i p(\vec{r})}{ik\rho_0 c}\Big)^*\Big\}, \quad (6)$$

where $*$ denotes the complex conjugate of the quantity, k is the wave number, ρ_0 the air density and c the velocity of sound.

For the normal intensity vector, eq. (6) is rewritten in the following form:

$$I_n(\vec{s}) = -\frac{1}{2}\Re e\Big\{p(\vec{s})\Big(\frac{\partial_n p(\vec{s})}{ik\rho_0 c}\Big)^*\Big\}, \quad (7)$$

where the minus sign is added to be conform with the vizualisation of vector flux direction. An outgoing flux is positive through a surface with the conventional outgoing normal. In our vizualisation map, this normal intensity becomes negative.

For the volumetric acoustic intensity vector maps, the intensity is computed on a lattice of points in Ω and displayed in three-dimensional plots, as shown in the next sections.

4 Numerical simulation

The mesh used in this numerical simulation is shown on figure 3, where the known quantities lie on the black surface (Γ^m) and the unknowns on the red one (Γ^u). This configuration has been chosen in order to fit the antenna used for the experimental part (see figure 7). The radius of the hemispheric antenna is $r = 0.15$ m. The total surface is discretized with 110 planar triangular elements and 57 nodes. There are 36 known double data (pressures and gradients), 21 unknown pressure data and 36 unknwon gradient data due to the joining curve where the surface is non-smooth. There are two different values of the gradient on a joining node because the normal is not the same for the two surfaces.

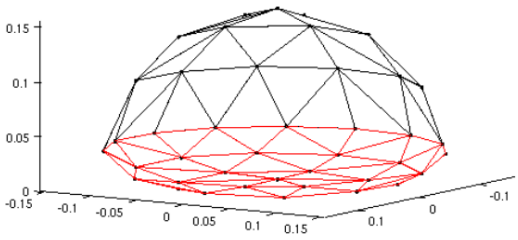

Figure 3: Mesh : Γ^m (black) - Γ^u (red).

The simulation test is a simple case. One places a monopole above the antenna for the first configuration ($\vec{r_0} = [0,0,1]$), below for the second one ($\vec{r_0} = [0,0,-1]$) and, for the last case, two monopoles at $\vec{r_1} = [1,0,1]$ and $\vec{r_2} = [1,0,-1]$. This last configuration tests the method when the antenna is placed near a rigid wall without source in front of it. The Γ^u surface is approximately on the (x,y) plane (see figure 3). Figures (4) to (6) show on the left the theorical intensity map and on the right the results of the DCM. In these figures, the normal intensity is scaled in dB and the color of the intensity vectors is proportional to its linear magnitude. One can see that when the source is above or below the antenna, the results of the DCM are a little more concentrated in the center of the Γ^u surface where the maximum and minimum levels are increased by approximately 1 dB. To improve the accuracy, different designs of the antenna must be tested and perhaps increased the order of the shape fonctions used on the numerical implementation of the integral formulations. The essential conclusion drawn from these figures is that the direction of the point source is correctly indicated by the intensity vectors. When the antenna is placed in front of a rigid surface, corresponding of the third case, the figure 6 shows that the intensity vectors are parallel to the (x,y) plane.

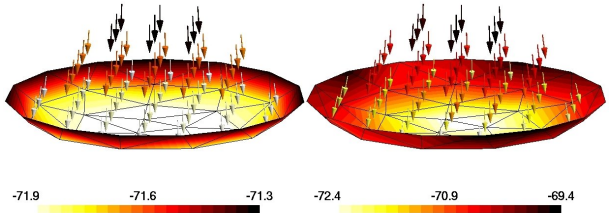

Figure 4: Theorical (left) and calculated (right) active intensity at 300 Hz, monopole on top ($z = 1$ m).

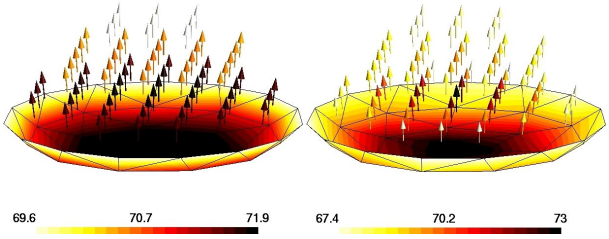

Figure 5: Theorical (left) and calculated (right) active intensity at 300 Hz, monopole below ($z = -1$ m).

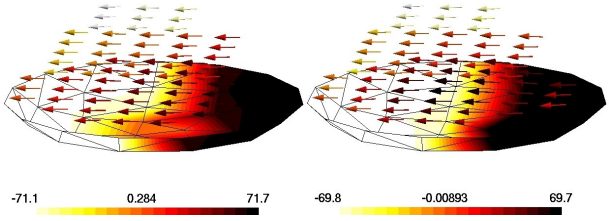

Figure 6: Theorical (left) and calculated (right) active intensity at 300 Hz, monopoles at $\vec{r_1} = [1,0,1]$ and $\vec{r_2} = [1,0,-1]$.

5 Experimental results

Figure 7 shows a photography of the antenna used in the experiments. On this antenna, 36 p-p probes are fixed to form an hemispheric surface. The lenght of inter-space between the microphone is 3 cm (see figure 8). Proper calibration is performed to correct modulus and phase mismatch between microphones. The mock-up is a nearly rectangular box with a slanting face. The size of the mock-up is about (0.85/0.75 m $\times$ 1.1 m $\times$ 0.7 m). The picture shows loudspeakers, but there are not used in this configuration test. One uses a shaker fixed at the handle of one small vertical face of the mock-up (see figure 9). The antenna is moved on 14 positions in the box: 2 positions in front of each short vertical faces, 3 positions in front of the long vertical face, 3 positions in front of the slanted long vertical face and 4 positions in the bottom face. The upper face is not easily accessible and no position has been taken on it.

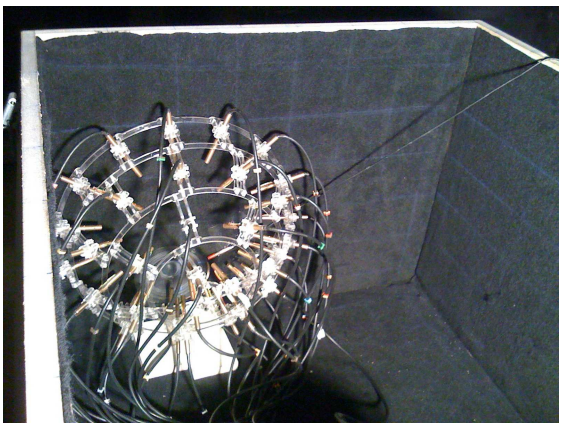

Figure 7: Antenna installation in mock-up.

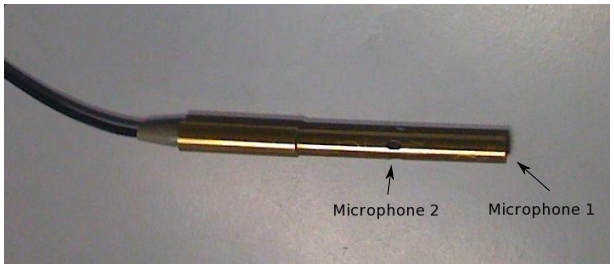

Figure 8: Example of a p-p probe.

Figure 10 shows the superposition of the power spectrum of an accelerometer placed near the shaker (black line) and the mean power spectrum over all pressure points in the mock-up (grey line). The pics on each response correspond to acoustical and structural modes. The frequency of 165 Hz corresponds to an antiresonance where the response of the accelerometer is minimum in contrast of a high level of pressure in the box.

In the figures 11 to 16, we present for each frequency the pressure map and the results of the data completion method. The pressure map is formed by the 14 positions of the antenna in the box. The shaker drive voltage (a pseudo band-pass signal between 20 and 3000 Hz) is used as the reference signal to calculate the transfert functions. 150 nonoverlapping segments of time record, each containing 512 points,

Figure 9: Picture of the mock-up.

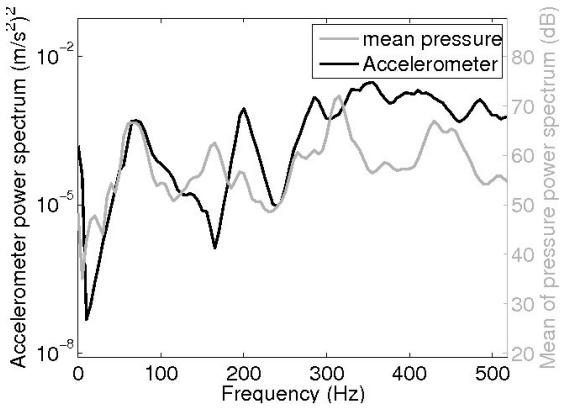

Figure 10: Superposition of accelerometer and pressure power spectrums.

are used with a sample rate of 5120 Hz. In order to compensate the nonstationarity between the 14 mesurements, an average is performed on the 14 auto-spectral references to yield complex pressure:

$$p_y = H_{ry}^{step} \times \sqrt{S_{rr}^{avg}} \tag{8}$$

where H_{ry}^{step} is the transfert function between one microphone and reference for one antenna position and S_{rr}^{avg} is the average of the 14 auto-spectral vectors of the reference. This procedure yields smooth pressure maps.

The results of DCM is the representation of the normal active intensity on the surface Γ^u and the vectors of active intensity inside the antenna domain (empty domain Ω) for the 14 positions. For a better visualization, only the higher levels are represented: positive values in red scale and negative values in yellow scale with 10 dB of dynamic range each. As in the previous simulation part, negative intensities mean that there is a flux flowing out of the structure of the mock-up. The intensity vector representation is an helpfull tool to localize the most vibrating surfaces. In contrast, when these vectors are parallel to the surface, that means that the structure doesn't vibrate.

Figures 11 and 12 show results at 70 Hz. The measured pressure is quite homogeneous (6 dB of dynamic) with a maximum near a corner. In fact, this maximum is at the opposite side of the source point excitation as we can see on figure 12. On this figure, we clearly identify the excited face

of the mock-up. Three faces have positive normal active intensities, the long vertical face has a negative one and the bottom face seem to be rigid. We can identify on this figure that the structure moves on an acoustical mode (0,0,0) in the box.

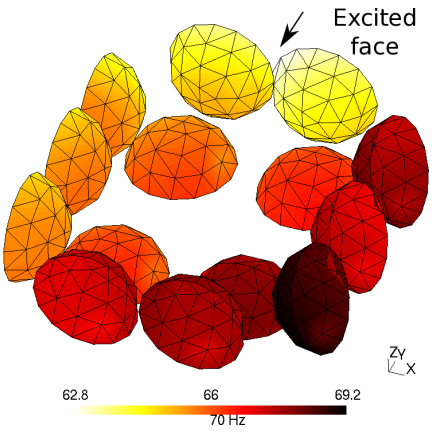

Figure 11: Measured pressure at 70 Hz.

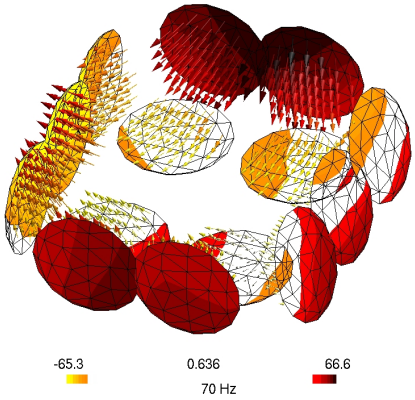

Figure 12: Calculated active intensity at 70 Hz

Figures 13 and 14 show results at 195 Hz. The pressure map corresponds to the acoustical mode (1,0,0) in the box. On the intensity map, one recognizes a (1,0) plate mode on the excited face: one side has positive values with ingoing intensities and the other has negative values with outgoing vectors. We see also that the long vertical face is excited near the corner.

Figures 15 and 16 show results at 315 Hz. The pressure map corresponds to the acoustical mode (0,2,0) in the box. On the intensity map, one recognizes a (2,0) plate mode on the excited face: there is a negative area between two positives. The others face, where intensity vectors are parallels to the structure, seem to be rigid.

Figures 17 and 18 show results at 165 Hz. The pressure map shows the (0,1,0) acoustical mode in the box. On the intensity map, one can see that the opposite face vibrates on his (1,0) plate mode. There is a coupling between the two opposite plates where the opposite face vibrates more than the excited face. This has been previously seen on the accelerometer power spectrum which shows an antiresonance reponse at this frequency.

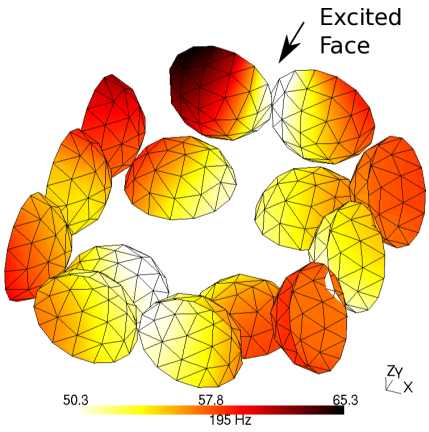

Figure 13: Measured pressure at 195 Hz.

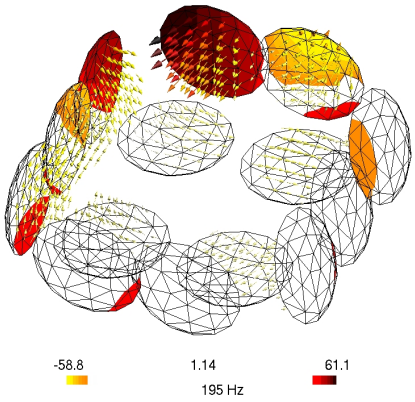

Figure 14: Calculated active intensity at 195 Hz

6 Conclusion

This paper presents an experimental application of the Data Completion Method (DCM) for acoustic imaging. From a set of acoustical quantities (pressure and velocity) on a boundary part of an empty domain, one can access to the set on the remaining part. This is a more general approach to resolve the inverse problem in acoustic. The advantage of this formulation is that it works even if sources are all around the antenna and not only in front of it. This is an alternative method for confined domain where usual imaging methods fail to give a solution.

The results show that this is a very efficient method at low frequencies. In this case, from the pressure map it is impossible to localize the origin of noise. The DCM is a powerfull method to evaluate the vibration of structure with intensity vector map. This is an helpfull technique to understand the vibro-acoustic problem.

Another important point is that the DCM use a local geometry which allows to perform only measurements around a source without modelling the entire geometry. This fact is important in balance to the time consuming of the algorithm. Once the numerical integrals are performed, they can be stocked for a geometry and can be used after for several cases. In this paper, our geometry is suitable to perform measurement near a plane structure. In future works, other antenna designs will be studied to test different geometries, for example near an edge or a corner, where it is difficult to have

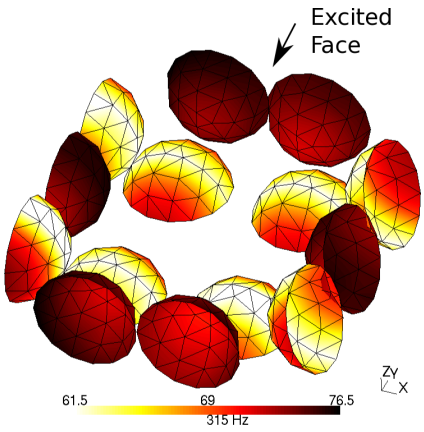

Figure 15: Measured pressure at 315 Hz.

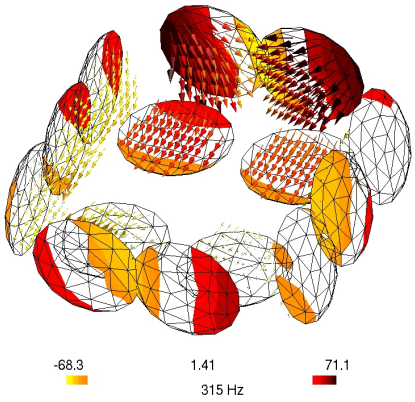

Figure 16: Calculated active intensity at 315 Hz

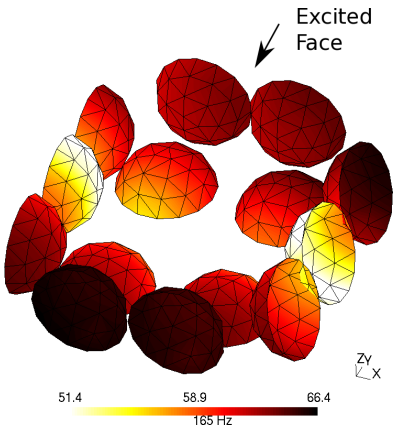

Figure 17: Measured pressure at 165 Hz.

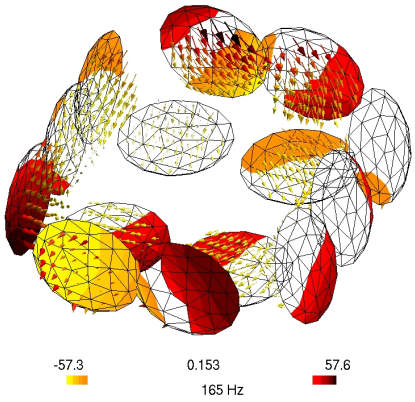

Figure 18: Calculated active intensity at 165 Hz

results with classical methods.

References

[1] C. Langrenne and A. Garcia, “Le problème inverse acoustique vu comme la solution d’un problème de Cauchy associé à l’équation de Helmholtz”, actes du 10ème Congrès Français d’Acoustique, CFA 2010, Lyon, France, 12-16 avril 2010.

[2] C. Langrenne and A. Garcia, “ Data completion method for the characterization of sound source”, J. Acoust. Soc. Am. **130** (4), october 2011, 2016-2023.

[3] S. F. Wu, “Methods for reconstructing acoustic quantities based on acoustic pressure measurements”, *J. Acoust. Soc. Am.* **124** (5), 2680-2697 (2008).

[4] A. F. Seybert, B. Soenarko, F.J. Rizzo and D.J. Shippy, “An advanced computational method for radiation and scattering of acoustic waves in three dimensions”, *J. Acoust. Soc. Am.* **77**, 362-368 (1985).

[5] P. C. Hansen, “Analysis of discrete ill-posed problems by means of the L-curve”, *SIAM Rev.* **34**, 561-580 (1992).